Model-Based Detection of Hydrogen Leaks in a Fuel Cell Stack

Ari Ingimundarson, Anna G. Stefanopoulou, and Denise A. McKay

***Abstract*—Hydrogen leaks are potentially dangerous faults in fuel cell systems that are fed with hydrogen-rich gas mixtures. This brief presents an approach to hydrogen leak detection and, thus, complements direct detection using hydrogen sensors. It relies on simple mass balance equations of an anode filling volume after taking into account the natural leak of the stack. A hydrogen mass flow, anode pressure, and relative humidity sensor are employed. Hydrogen leak detection without the use of relative humidity sensors is considered by employing adaptive alarm thresholds to eliminate false alarms. The validity of the method is also discussed in terms of common hydrogen supply system configurations. The detection method is validated using a 1.25-kW polymer electrolyte membrane fuel cell stack in a laboratory facility where leaks could be introduced in a controlled manner.**

***Index Terms*—Fault diagnosis, fuel cells, hydrogen leak, safety.**

I. Introduction

A COMMON safety concern for fuel cell systems is hydrogen leaks [1]. As hydrogen is a flammable gas that requires extremely small ignition energy, its uncontrolled and undetected release in confined nonventilated spaces carries risks. In [2], the safety characteristics associated with hydrogen are compared to other common fuels. Hydrogen has the lowest molecular weight and viscosity of any gas; thus, it has a faster leak rate through small orifices [3] and is more difficult to contain. In hydrogen-fed fuel cell stacks, there is always an accepted leak rate, as it is extremely difficult and expensive to completely seal the stacks. An increased leak rate due to cracks in the graphite plates, seal ruptures, or membrane cross-leaks could cause a critical concentration of H_2 to accumulate leading to an explosion.

The standard solution to hydrogen leak detection is to install hydrogen sensors at strategically selected places close to the fuel cell stack and/or submit the system to periodic inspections. Fast hydrogen sensors with high sensitivity, wide range, and long-term stability are under intensive development [4]. Periodic inspections are subjective and incapable of detecting sudden changes in leak rate. As a result, automated ways of detecting leaks that complement direct detection using hydrogen sensors are of interest.

Manuscript received September 15, 2006. Manuscript received in final form October 3, 2007. First published March 31, 2008; last published July 30, 2008 (projected). Recommended by Associate Editor S. Palanki. This work was supported in part by the Ramon y Cajal program, in part by the CICYT project DPI2005-05415 of the Spanish government, in part by the Research Commission of the "Generalitat de Catalunya" (group SAC ref.2001/SGR/00236), in part by the U.S. National Science Foundation, and in part by the Ford Motor Company.

A. Ingimundarson is with the Automatic Control Department, Campus de Terrassa, Technical University of Catalonia, Rambla Sant Nebridi, 10, 08222 Terrassa, Spain (e-mail: ari.ingimundarson@upc.edu).

A. G. Stefanopoulou and D. A. McKay are with the Fuel Cell Control Laboratory, Mechanical Engineering, University of Michigan, Ann Arbor, MI 48109 USA (e-mail: annastef@umich.edu; dmckay@umich.edu).

Digital Object Identifier 10.1109/TCST.2007.916311

This brief shows how hydrogen leaks on the anode side of a fuel cell can be detected using existing sensors commonly used for control in addition to a mass flow meter in a pure hydrogen polymer electrolyte membrane (PEM) fuel cell stack. Leak detection of gases has been studied by [5] as part of a diagnostic system for the air path of an automotive diesel engine. The boost pressure in a diesel engine is similar to the anode (hydrogen-side) and cathode (air-side) of a PEM fuel cell, operating at 100–200 kPa. An important difference between the problem in [5] and the one addressed here is that the estimation of the hydrogen leak rate must take into account the presence of water vapor in the anode. Sections III and IV show the leak detection algorithm employing a relative humidity sensor for real-time measurement of the anode relative humidity.

Apart from the increased cost of using a relative humidity sensor, anode leak detection presents additional challenges associated with the spatial variability of water partial pressure in the anode channels of a fuel cell stack. Water partial pressure in the anode can vary spatially in the stack from zero (dry) to the saturation pressure (fully humidified). However, the reaction of hydrogen and oxygen at the cathode generates water vapor which diffuses through the membrane to the anode. Thus, water vapor will always be present in the anode. Anode humidity becomes important as membranes become thinner due to the increased membrane water mass flux associated with thinner membranes. The water vapor partial pressure can also change significantly during operation, especially when the anode is purged periodically. Purging of the anode gases is a common solution to remove liquid water and inert gas, such as nitrogen, from the membrane and gas channels [6]. As the total gas leak is assumed to depend on the pressure difference between the anode and the surroundings, the hydrogen leak will depend on the composition of the gas where the leak occurs. Our approach in Section V is to use the fact that the water vapor partial pressure is bounded by the saturation pressure to create adaptive alarm thresholds when the anode humidity is not measured.

The presented work also has many similarities to [7], where an observer was designed to estimate anode hydrogen pressure with an output-injection term based on stack voltage. In [8], additional flow and pressure measurements were used to estimate the partial pressure of hydrogen as there are many phenomena that can affect stack voltage besides hydrogen pressure.

In this brief, two leak detection quantities are presented and their advantages and disadvantages are compared. A detection quantity is simply a scalar value calculated from process data that refutes the validity of assumptions associated with it. The detection quantity is refuted if it rises above a predetermined threshold. The main assumption that the presented detection quantity refutes in the current article is that no leak is present, see [9]. Exact interpretation of the detection quantities will be presented in Section III. Detection quantities are also referred to as analytical redundancy relations (ARR).

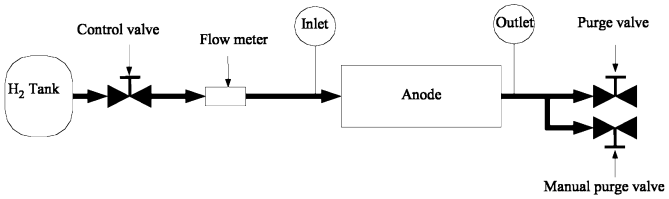

Fig. 1. Configuration of the hydrogen supply system.

The main requirements for leak detection is swift and reliable detection along with simplicity in evaluation. Sensor faults can be interpreted as leaks; therefore, the fewer sensors the detection method depends on, the better it will perform. This further justifies the focus on hydrogen leak detection without using relative humidity sensors.

A crucial sensor for the presented method is the hydrogen mass flow meter. Often such meters are not present in fuel cell configurations. The most common solution to control the amount of hydrogen in the anode is to control the anode total pressure with a pressure control valve or pressure regulator. On the other hand, a hydrogen mass flow meter might be used for other failure detection algorithms or fuel economy calculations.

In Section II, the experimental set-up used to calibrate and validate the proposed algorithm is introduced. Then the model of the fuel supply subsystem is presented. In Section III, the detection quantities are introduced. In Section IV, the model and detection quantities are experimentally validated. In Section V an adaptive threshold is introduced to take into account the error in the detection quantities when relative humidity is unknown. Section VI discusses the validity of the detection quantities for common hydrogen supply system configurations. Finally, in Section VII, some conclusions are drawn.

II. Background and Modeling

The detection quantities introduced depend on a comparison of the estimated rate of change of mass in the anode using two different sets of measurements, namely, mass flow rates and pressure. The first quantity detects the hydrogen mass flow rate leaking from the anode. The second quantity detects changes in the leak area through unaccounted flow leaking out of the anode. Before introducing the specific parity equations, the model equations are presented. Control-oriented models are typically low-order models used in real-time calculations with embedded computational hardware. These models need to be simple for fast computations and require many assumptions that need to be experimentally calibrated and validated. Thus, we start by presenting the experimental configuration used for model detection calibration and validation.

A. Experimental System Configuration

In Fig. 1, a schematic diagram of the components relevant to hydrogen leaks is shown. Since failures are most often related to physical components, it is important when designing failure detection algorithms to be aware of the physical components that the model equations represent.

The fuel subsystem supplies hydrogen gas at a desired pressure to the fuel cell stack. Dual-stage and low-pressure regulators are used to reduce the hydrogen tank pressure to a desired anode inlet total pressure. The hydrogen gas then enters the dead-ended anode that is occasionally purged using either a manual or solenoid valve.

The stack used for this investigation has 24 PEM fuel cells with 300-cm^2 active surface area, GORE PRIMEA membrane electrode assemblies, and Etek ELAT gas diffusion layers designed and assembled by the Schatz Energy Research Center at Humboldt State University for the Fuel Cell Control Laboratory at the University of Michigan. The stack can produce 1.25-kW continuous power at less than 400 mA/cm^2. It is designed for operation at low temperatures (< 70 C), and low gauge pressures (< 12 kPa in cathode and 14–34 kPa in the anode). The stack is water cooled and contains an internal humidification section that diffuses water vapor from the coolant to the incoming air. The hydrogen inlet gas is not humidified.

A Hastings HFM201 hydrogen mass flow meter, using hot wire anemometry, with a range of 0–100 slm ± 1 slm, and a response time of 2 s is installed upstream of the anode inlet. Temperature sensors (thermocouples) with an accuracy of $\pm 0.03[K]$ are placed in the anode inlet and outlet manifolds. Sensors are placed in the inlet and outlet manifolds due to the difficulties associated with embedded measurements at a stack level. A common approximation is to assume the temperature varies linearly between the inlet and outlet of the electrode. Due to the typical dead-ended anode operation, a pressure sensor placed in the anode is sufficient for inferring an overall anode total pressure. An Omega PX4202–005G5V pressure transducer with a range of 0–5 psig, an accuracy of ± 0.012 psig, and a response time of 10 ms was used. Relative humidity (RH) is very difficult to measure due to the formation of liquid condensation in the electrodes. Using the model in [10] and off-line experiments with RH sensors (Rotronic SP05 probes), we established a lookup table for the mean anode humidity at different loads (current drawn from the fuel cell), operating pressures, and temperatures.

The current drawn from the stack is controlled and measured by a Dynaload RBL488 electronic load with a range of 0–500 A (± 0.015 A). The data acquisition system is based on PCI DAQ boards with 5B Series signal conditioning hardware and LabVIEW software. Data logging occurs at 2 Hz or a higher frequency, depending on the task being executed.

B. Nomenclature

The following symbols appear in the model equations presented in this brief. Mass is denoted by m in [kg], mass flow rate by Q in [kg/s], pressure by p in [Pa], temperature by θ in [K], relative humidity by ϕ on the scale [0–1], and molar mass of element i by M_i [kg/mole]. The subscript H_2 is used for hydrogen, w for water vapor, an for anode, nl for natural leak, and atm for atmosphere. $I_{\rm st}$ in [Amper] is the stack current, $F = 96485.3415$ is the Faraday constant [Coulomb/mole], n is the number of cells, and x and y are mass and molar fraction respectively. Anode volume is denoted by $V_{\rm an}$ and is equal to 0.00055 m^3.

C. Detection Model Equations

The detection model (DM) equations presented follow the work of [7], [8], and [11] for the rate of change of hydrogen and anode mass (m_{H_2} and $m_{\rm an}$) when no fault is present

$$\frac{dm_{H_2}}{dt} = Q_{H_2,\rm in} - M_{H_2}\frac{nI_{\rm st}}{2F} - Q_{H_2,nl} \quad (1)$$

$$\frac{dm_{\rm an}}{dt} = Q_{H_2,\rm in} - M_{H_2}\frac{nI_{\rm st}}{2F} - Q_{\rm nl} \quad (2)$$

where the mass rate of hydrogen consumed by the reaction associated with the stack current is the second term in the right hand side, $Q_{H_2,\rm in}$ is the measured mass flow of dry hydrogen supplied to the stack, and the mass flow of hydrogen, $Q_{H_2,\rm nl}$, due to the natural leak, $Q_{\rm nl}$, is calculated as

$$Q_{H_2,\rm nl} = x_{H_2}Q_{\rm nl} \quad (3)$$

where x_{H_2} is the mass fraction of hydrogen in the anode. The hydrogen mass fraction is estimated using the following equation:

$$x_{H_2} = \frac{p_{H_2,\rm an}}{p_{H_2,\rm an} + \frac{M_w}{M_{H_2}}p_{w,\rm an}} = \frac{p_{\rm an} - \phi_{\rm an}p_{\rm sat}(\theta_{\rm an})}{p_{\rm an} - \phi_{\rm an}p_{\rm sat}(\theta_{\rm an}) + \frac{M_w}{M_{H_2}}\phi_{\rm an}p_{\rm sat}(\theta_{\rm an})} \quad (4)$$

where $p_{\rm an}$ is the measured total anode pressure and the water vapor pressure is calculated using the measured anode humidity, $\phi_{\rm an}$, and the water vapor saturation pressure, $p_{\rm sat}$, which is a function of the measured anode temperature, $\theta_{\rm an}$.

The term $Q_{\rm nl}$ represents the natural leak from the anode of the fuel cell stack. This leak is always present due to the physical stack sealing design. It should be noted that the fuel cell used in this laboratory study has a larger natural leak rate than commercial fuel cell stacks. It is assumed that the natural leak is governed by a standard orifice relation through an effective area, $A_{\rm nl}$, that needs to be experimentally calibrated for each fuel cell stack system. Many companies that manufacture sealants, gaskets and other FC stack assembly components are currently exploring different models for gas leak rates, but have not reported a consensus yet. As we show in Section IV-B, the calibration of $A_{\rm nl}$ compensates for many modeling assumptions. The mass flow rate leaked from the anode is given by

$$Q_{\rm nl} = \frac{A_{\rm nl}p_{\rm an}}{\sqrt{R_{\rm an}\theta_{\rm an}}}(p_r)^{1/\gamma}\left(\frac{2\gamma}{\gamma-1}[1-(p_r)^{(\gamma-1)/\gamma}]\right)^{\frac{1}{2}} \quad (5)$$

where $p_r = p_{\rm an}/p_{\rm atm}$ is the pressure ratio across the assumed leak and the anode gas constant, $R_{\rm an}$, is calculated through the universal gas constant, R

$$R_{\rm an} = R/(y_{H_2}M_{H_2} + (1-y_{H_2})M_{H_2O}) \quad (6)$$

and the molar fraction of hydrogen in the anode

$$y_{H_2} = (p_{\rm an} - \phi_{\rm an}p_{\rm sat}(\theta_{\rm an}))/p_{\rm an}. \quad (7)$$

Additional variables λ and ψ are introduced to ease notation in Section III-B when the second detection quantity is introduced and Section V where the adaptive alarm limits for leak detection without humidity sensors are deduced. In particular, let λ be the term that depends on measured temperature and pressure such that (5) can be rewritten as

$$Q_{\rm nl} = A_{\rm nl}\lambda/\sqrt{R_{\rm an}}. \quad (8)$$

Then let ψ be a variable that isolates the effects of pressure, temperature, and humidity from the mass flow rate leaked

$$Q_{\rm nl} = A_{\rm nl}\psi. \quad (9)$$

We summarize here the assumptions associated with the detection model (ADM).

- ADM1: For the anode control volume, (2) represents a simple mass conservation relation that neglects the water mass transport through the membrane.
- ADM2: For the hydrogen composition, it is assumed in (4) that there is no increased pressure due to liquid water accumulation, also known as flooding.
- ADM3: The nitrogen crossover is assumed to be negligible.
- ADM4: The leak can be modeled using an orifice equation without a separate hydrogen diffusion model.

These assumptions have been introduced because the models for the neglected quantities are too complex for fast computations and too difficult to calibrate using stack-level measurements [see [10] for modeled water mass transport through the membrane (ADM1), [12], [13] for the expected anode pressure variations during flooding conditions (ADM2), [14] for estimated nitrogen crossover (ADM3)]. In Section IV, we show validation results at three power levels after calibrating the natural leak area $A_{\rm nl}$.

Although the model in (1) and (2) represents a dead-ended anode fed by pure hydrogen, product water and inert gas (such as nitrogen) that diffuse from the cathode through the membrane are purged out of the anode by periodically opening a purge solenoid valve (see Fig. 1), causing a large but temporary increase in flow rate of hydrogen through the flow channel on the anode side, see [6]. The fault detection algorithms can be disabled during purging so the increased flow does not cause a false alarm.

III. Detection Quantities

A common way to select detection quantities is to use a measurement and a model prediction of that measurement and form a quantity that expresses the distance between the two. The detection quantity is large if the model is refuted but zero otherwise.

A. Detection Quantity 1. Identification of Hydrogen Leak

The first detection quantity is formed by using Dalton's law of partial pressures, $p_{\rm an} = p_{H_2} + p_w$, and the ideal gas law $p_{H_2} = R_{H_2}m_{H_2}\theta_{\rm an}/V_{\rm an}$ and taking the time derivative on both sides

$$\frac{dp_{\rm an}}{dt} = \frac{dm_{H_2}}{dt}\frac{\theta_{\rm an}R_{H_2}}{V_{\rm an}} + \frac{d\theta_{\rm an}}{dt}\frac{m_{H_2}R_{H_2}}{V_{\rm an}} + \frac{dp_w}{dt}$$

with the hydrogen gas constant $R_{H_2} = R/M_{H_2}$. An additional assumption (ADQ1) is introduced for establishing detection quantity 1.

- ADQ1: The time derivatives of water vapor pressure and temperature are neglected as they are usually much smaller than the other terms.

The rate of change of temperature is much slower than the dynamics in pressure and mass flow rate as can be seen later in Fig. 3. In the case of an internal membrane type humidifier, the humidity dynamics follow the temperature dynamics. When the humidity of hydrogen entering the stack is actively controlled, for example by steam injection, this assumption should be verified carefully. Solving for the mass derivative and moving all terms to the right side of the equation, one obtains as a detection quantity

$$T_1(t) = \frac{dm_{H_2}}{dt} - \frac{V_{\rm an}}{\theta_{\rm an} R_{H_2}} \frac{dp_{\rm an}}{dt}. \tag{10}$$

The time derivative of m_{H_2} is replaced by expression (1). The measurement sample time is 0.5 s. The numerical derivative of the anode pressure is implemented as suggested in [15] with a first-order low pass filter. The filter time constant was chosen as 2 s. The hydrogen mass flow meter has a 2-s response time, so that signal was not filtered. Using $\bar{(\cdot)}$ for measured and $\hat{(\cdot)}$ for estimated or modeled signals, the detection quantity is calculated as

$$\begin{aligned} T_1(t) &= \frac{d\hat{m}_{H_2}}{dt} - \frac{V_{\rm an}}{\bar{\theta}_{\rm an} R_{H_2}} \frac{d\bar{p}_{\rm an}}{dt} \\ &= \bar{Q}_{H_2,\rm in} - M_{H_2} \frac{n\bar{I}_{st}}{2F} - \hat{Q}_{H_2,nl} - \frac{V_{\rm an}}{\bar{\theta}_{\rm an} R_{H_2}} \frac{d\bar{p}_{\rm an}}{dt} \end{aligned} \tag{11}$$

which should be 0 when the only leak is the natural leak from the fuel cell stack ($\hat{Q}_{H_2,nl} = Q_{H_2,nl}$) or when the estimated hydrogen leak ($\hat{Q}_{H_2,nl} = \hat{A}_{\rm nl} \bar{\lambda} \bar{x}_{H_2} / \sqrt{\bar{R}_{\rm an}} = A_{\rm nl} \bar{\lambda} \bar{x}_{H_2} / \sqrt{\bar{R}_{\rm an}}$) through the modeled natural leak $\hat{A}_{\rm nl}$ is equal to the actual hydrogen leak.

Checking the T_1 value during no fault conditions is an indirect validation of the model and the detection quantities' assumptions (ADM1-4 and ADQ1, respectively). Small T_1 values during no fault conditions justify the modeling assumptions as shown in Section IV-B.

Therefore, this detection quantity monitors the rate of change in anode pressure and checks if this change corresponds to an inbalance between the hydrogen influx versus the rate of consumption and the modeled natural leak. If T_1 is nonzero or greater than a threshold value that is determined based on the expected modeling error at different operating conditions, we attribute the mismatch in the two mass flow rates to a hydrogen leak $Q_{\rm fault}$ beyond the modeled natural leak. In fact, T_1 is an estimate of the increase in hydrogen leakage ($T_1 = Q_{\rm fault}$) in units of [kg/s].

B. Detection Quantity 2. Identification of Change in Leak Area

A common approach to failure detection of a process is to identify its parameters and see if they remain on a prescribed interval. If the parameter leaves the interval, a fault has occurred, see [16]. The second detection quantity utilizes this approach. We assume that any increase in the anode leak rate can be expressed as an increase in the leak area $Q_{\rm fault} = \Delta A_l \psi$. An estimate is created of the change in the leak area, ΔA_l, from the natural leak area, $A_{\rm nl}$. See [17] for a reference where a similar approach was presented.

One of the main advantages of this detection quantity is that it returns a quantification of the increase in leak area. If, during operation, the fuel cell is subjected to large pressure differences, a certain increase in leak area detected at low pressure could avoid dangerous situations at higher pressures when a larger leak area would lead to a larger hydrogen leak.

Detection quantity 2 is formed in a similar way as detection quantity 1. Using an expression of the ideal gas law for the anode pressure, $p_{\rm an} = R_{\rm an} m_{\rm an} \theta_{\rm an} / V_{\rm an}$, and taking a time derivative on both sides, the following expression is formed:

$$T_2(t) = \left(\frac{dm_{\rm an}}{dt} - \frac{V_{\rm an}}{\theta_{\rm an} R_{\rm an}} \frac{dp_{\rm an}}{dt} \right) / \psi \tag{12}$$

$$= \Delta A_l. \tag{13}$$

The time derivative of the anode mass is calculated using (2). The time derivative of temperature is again assumed to be small compared to the other terms.

When the pressure in the anode approaches atmospheric, the term ψ approaches zero, causing the estimate for ΔA_l to be untrustworthy. This detection quantity might, therefore, have limited validity, especially at startup and shutdown when pressure in the anode is close to atmospheric.

C. Interpretation of Detection Quantities

Related to each detection quantity is a set of components on which the equations are based. Following the framework presented in [18], if all components are functioning normally, the detection quantities will not deviate from an interval around zero. These intervals correspond to lower and upper thresholds for the detection quantities. The size of the intervals are determined from noise and model uncertainty (see Section IV). If the detection quantity rises above the upper limit, it is assumed that at least one of the components is not functioning normally. A possible failure in this case is an increase in leak area resulting in an increase in the hydrogen leak. If a detection quantity drops below its threshold, at least one of the components is not functioning normally. However, an increase in leak area is excluded from the list of possible faults as the fault parameter ΔA_l affects each detection quantity positively. Notice it is not assumed that if the detection quantities are inside of their intervals, all components are functioning normally. The detection quantities only invalidate assumptions related to them.

As there are a number of components related to each detection quantity, one cannot directly assume that a hydrogen leak is present when a detection quantity rises above the threshold without further information. It is assumed that other faults have been considered less probable either with hardware redundancy, by probabilistic arguments about other components (failure rate of sensors), or by construction of other detection quantities. From this argument, it is clear that the fewer components that support a detection quantity the better.

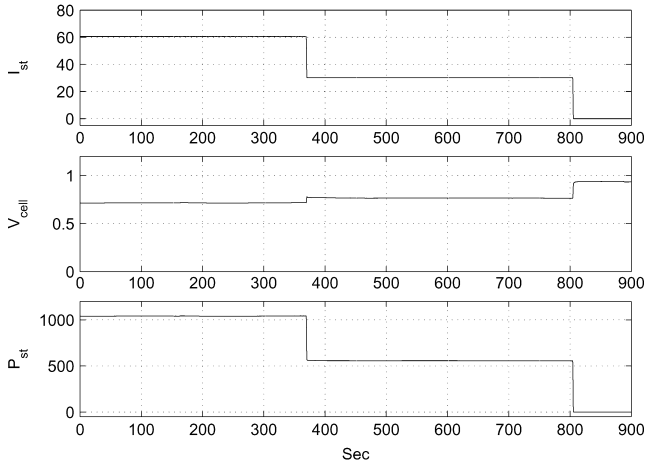

Fig. 2. Stack current $I_{\rm st}$ [Amp], average cell voltage $V_{\rm st}$ [Volt], and stack power $P_{\rm st}$ [W] for the data series considered.

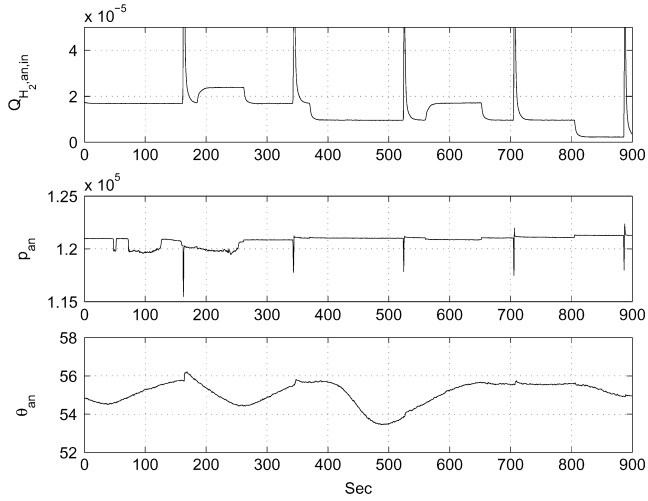

Fig. 3. Hydrogen mass flow $Q_{H_2,\rm in}$ [kg/s], anode pressure $p_{\rm an}$ [Pa], and anode temperature $\theta_{\rm an}$ [°C] for the data series considered.

IV. Validation

The presented detection quantities should equal zero when no fault is present. Any discrepancy from zero is due to model errors and measurement noise. As these error sources will always be present, it is vital to test the detection quantities without fault over as many operating regions as possible to determine the interval that the detection quantities stay on in the fault free case.

A. Experiments

The detection quantities were calculated for the experiment shown in Figs. 2 and 3. During this experiment, two stack power levels were tested as shown in Fig. 2. In the last part of the data series, no current is drawn from the stack. The graph of the hydrogen flow requires further explanation. The spikes at times 162, 343, 524, 705, and 886 s in hydrogen mass flow and anode pressure are due to anode purging as mentioned in Section II. The slower rise at times 185 and 560 s are due to leaks that were provoked by opening the manual purge valve. Furthermore, the variations in anode pressure at times 50–250 s occurred due to a fault in the anode pressure sensor. We show later that these variations were so small they had no effect on the calculation of the detection quantities. Finally, with a series of independent RH measurements [20] and estimation through a calibrated water mass transport model [19], the anode was found to be partially drying with 50% anode humidity at the high power level (60 A) and fully humidified (100% RH) at 40 A and zero load.

B. Model Validation

After calibrating the model by determining the natural leak rate, the detection quantities T_1 and T_2 should be zero for all the conditions except when a fault (additional hydrogen leak) occurs. Equation (11) is used at selected periods, when steady state conditions can be assumed, to calculate the stack natural leak, $Q_{\rm nl}$, that is found in the range of $[1.8\text{–}2.2] \cdot 10^{-6}$ kg/s. The variation is due to unmodelled quantities associated with assumptions ADM1-4 and ADQ1 or from the hydrogen mass flow sensor nonlinearities and resolution at low hydrogen mass flow rates (low load). The modeled natural leakage of the stack was selected to be $Q_{\rm nl} = 1.8 \cdot 10^{-6}$ kg/s, the value predicted at high power. Using (5) with 50% RH in (6) and (7), the modeled natural leak area is calculated as $A_{\rm nl} = 2.4 \cdot 10^{-8}$ m^2.

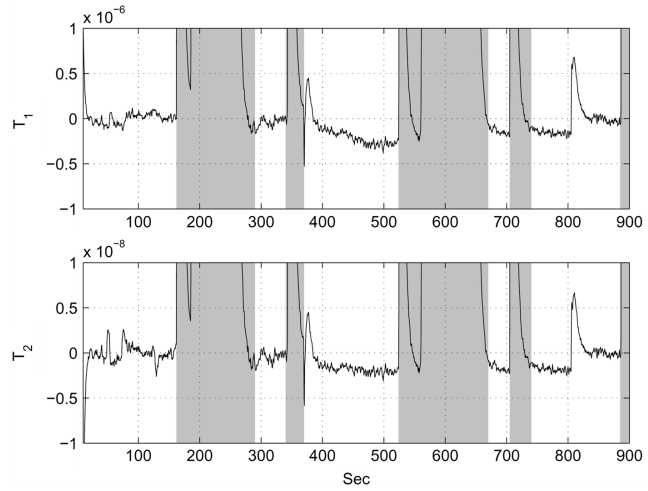

Fig. 4. Detection quantities calculated for the data series. Grey areas should be discarded due to purging or provoked leaks. The detection quantities in the remaining regions serve as a model validation after the calibration of the natural leak.

As mentioned above, the natural leak of the stack used in the reported experiments is larger than the natural leak of commercially available stacks. Note here that a natural leak rate of $2 \cdot 10^{-6}$ kg/s corresponds to a volumetric flow rate of $24.2 \cdot 10^{-6}$ m^3/s (using 0.0827 kg/m^3 for hydrogen density at 20 °C and 100 kPa). A garage with dimensions $5 \times 4 \times 3$ m$= 60$ m^3 reaches the 4% lower flammability limit (LFL) [14] when the volume of hydrogen leaked is 2.4 m^3. A simple calculation shows that it would take approximately 28 h, if the garage remains unventilated throughout this time period, for the LFL to be reached. If a hydrogen gas sensor were installed to alarm at 1% LFL (a typical threshold), the leak would persist for 7 h before a fault were triggered.

The maximum error of T_1, when no leak is present, occurred at 810 s when the current dropped from 30 A to 0 and was equal to around $7 \cdot 10^{-7}$ kg/s, as shown in Fig. 4. The maximum error

TABLE I
SENSITIVITY OF DETECTION QUANTITIES FOR EACH SENSOR

z Unit	$\bar{Q}_{H_2,\text{in}}$ [kg/sec]	$\bar{I}_{st}$ [A]	p_{an} [Pa]	θ_{an} [K]
Δz	$\pm 1.3 \cdot 10^{-6}$	± 0.015	± 100	± 0.03
ΔT_1	$1.3 \cdot 10^{-6}$	$3.7 \cdot 10^{-9}$	$2.5 \cdot 10^{-10}$	$4.1 \cdot 10^{-11}$
ΔT_2	$1.8 \cdot 10^{-8}$	$5.1 \cdot 10^{-11}$	$5.4 \cdot 10^{-10}$	$3.1 \cdot 10^{-10}$

of T_2 was observed at 810 s and was estimated to be around $7 \cdot 10^{-9}$ m^2. Notice that the maximum error of both detection quantities occur when there is a change in power output. At stationary conditions, the error in the detection quantities is small, even though the fuel cell is operating under different conditions.

A sensitivity analysis was performed to estimate the effect of sensor error on the detection quantities. The effect was estimated by calculating

$$\Delta T_i = \max_{\delta=\{\Delta z, -\Delta z\}} |T_i(\cdot, z) - T_i(\cdot, z+\delta)| \tag{14}$$

for each sensor z used in (11) and (12), for the experiment presented, using the sensor accuracy Δz reported in Section III-A. The maximum values obtained for the whole experiment are reported in Table I. It can be seen that the sensor whose accuracy has most impact on the detection quantities is the hydrogen mass flow meter. The error in the detection quantities due to this sensor is in the order of magnitude of the error of T_1 and T_2 reported before.

It should be noted that the sensors usually have much better repeatability than accuracy. The mass flow meter has a repeatability of $\pm 6.8 \cdot 10^{-8}$. Lower error in the test quantities can, therefore, be expected close to the operating point where A_{nl} is calibrated. A_{nl} was calibrated at high power, causing the error of the test quantity to be smaller at intervals 0–163 and 300–340 than expected from the sensitivity analysis. The first interval also contains the effect of the failure in the pressure sensor.

The unmodeled effects of the accumulation of nitrogen and water in the anode do not appear to be significant from inspection of the detection quantities. During a purge, nitrogen and water, transported through the membrane from the cathode, are removed from the anode. However, the detection quantities are approximately equal before and after a purge. Any modeling error due to this accumulation should be present in the detection quantity, further validating our assumption in ADM3.

C. Leak Detection

In Fig. 5, the detection quantities are shown again for the data series but with a different scale on the y-axis. The scale of each detection quantity is different by orders of magnitudes as they measure different physical quantities. T_1 directly measures the leak rate in [kg/s] and can be compared to the actual hydrogen usage in Fig. 3. It can be seen in Fig. 5 that the detection quantity rises to around $6 \cdot 10^{-6}$ kg/s when the leak was provoked with the manual valve at 185 and 560 s. This corresponds to approximately three times the natural leak.

T_2 on the other hand measures the increase in leak area. This graph can be compared to the natural leak area, A_{nl}, which was calculated as $2.4 \cdot 10^{-8}$ m^2. The graph shows that ΔA_l increases to about $7 \cdot 10^{-8}$ m^2 when the leak occurs, approximately three times the natural leak area.

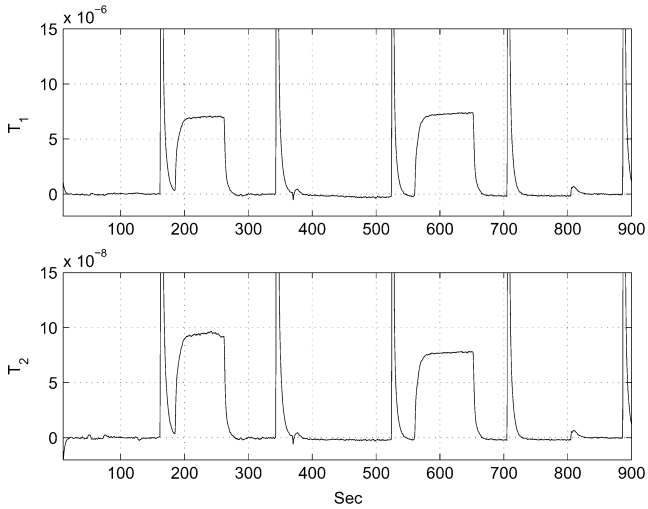

Fig. 5. Detection quantities calculated for the data series.

It is important to note again here that the algorithm should be considered as a redundant hydrogen leak detection method that measures leak rate primarily to complement detection with hydrogen gas sensors that measure the percent hydrogen contained in a volume. The algorithm should be able to detect leaks larger than three times the modeling error (3×1 mg/s) within a few seconds (computational time depending on the algorithm implementation and sensor response time). In contrast, a 3 mg/s hydrogen leak rate (continuous flow) in a 60 m^3 unventilated garage space will trigger the hydrogen detection and associated hardware alarm system within 4.6 h, assuming the hardware hydrogen detection (hydrogen sensor) has been calibrated and issues an alarm when the volumetric hydrogen concentration reaches 1% LFL. Thus, the proposed algorithm could provide an early warning (within seconds) of a potential leak that could cause shutdown within 4.6 h or could approach explosive limits within 18.4 h if unattended.

V. HYDROGEN LEAK DETECTION WITHOUT USING HUMIDITY SENSORS

Simplifications will be presented for the detection quantities which aim at terminating dependence on the relative humidity sensors. Notice that the two detection quantities presented depend on all components (sensors) discussed in Section II. Omitting sensors causes errors in the detection quantities as the previously measured variable is not known but has to be estimated or replaced by a constant.

The effect of relative humidity on the detection quantities appears through the mass fraction term in (4) and the anode gas constant in (6). Relative humidity varies spatially and temporally within the anode. As mentioned before, the relative humidity can vary spatially due to the supplied humidity conditions as well as the membrane vapor transport. Anode humidity can vary in time due to singular events, such as anode purging, or transient effects during load changes. Second, the exact location of the natural leak is unknown. The total leak might be composed of various smaller leaks distributed over the stack. These two facts make the exact determination of variables that

depend on relative humidity, such as the mass fraction, x_{H_2}, and anode gas constant, R_{an}, difficult to determine in practice.

An error in the estimation of these variables can cause false alarms or missed detections when using the detection quantities presented. A false alarm can occur when the relative humidity is overestimated, as the natural leak of hydrogen will be larger than assumed without an increase in the natural leak area, A_{nl}. Additionally, an increase in the natural leak area can go undetected if the relative humidity is underestimated. On the other hand, relative humidity is a physical parameter, bounded to the interval [0,1]. This can be exploited to estimate the maximum error in the detection quantities if a specific relative humidity is assumed.

Assume that the first detection quantity is calculated with relative humidity ϕ_1 when the real relative humidity is ϕ_2. For ease of notation, the detection quantities are written only as functions of relative humidity in what follows. The maximum error due to this mismatch is

$$\begin{aligned}\Delta T_1 &= \max_{\phi_1,\phi_2\in[0,1]} T_1(\cdot,\phi_1) - T_1(\cdot,\phi_2) \\ &= \max_{\phi_1,\phi_2\in[0,1]} -A_{\text{nl}}\left(\frac{x_{H_2}(\phi_1)}{\sqrt{R_{\text{an}}(\phi_1)}} - \frac{x_{H_2}(\phi_2)}{\sqrt{R_{\text{an}}(\phi_2)}}\right)\lambda.\end{aligned} \tag{15}$$

Tedious but straight forward calculations show that $x_{H_2}(\phi)/\sqrt{R_{\text{an}}(\phi)}$ is a monotonic function of ϕ on the interval [0,1]. Thus, the maximum ΔT_1 is achieved when the variables ϕ_1 and ϕ_2 are evaluated at the extremes of the interval [0,1]. The total expression of ΔT_1 is given in the Appendix where it is also shown how ΔT_2 can be estimated in a similar way as T_2.

The maximum error, ΔT, can be used as an adaptive alarm limit when the detection quantities are calculated without the relative humidity sensors. Notice that (15) implies that

$$T(\cdot,\phi) \geq T(\cdot,\phi_1) - \Delta T \quad \forall \phi \in [0,1].$$

The above statement in turn implies that if $T(\cdot,\phi_1)$ rises above ΔT, then $T(\cdot,\phi)$, calculated with the real ϕ, would rise at least as much above zero. Using $T(\cdot,\phi_1)$ as a detection quantity with ΔT as an alarm limit eliminates false alarms when relative humidity is unknown.

However, eliminating the risk of false alarms gives rise to the possibility of missed detections. As the maximum in (15) is achieved exactly for ΔT_1, the adaptive alarm limit serves to quantify the maximum leak rate that could go undetected when $T(\cdot,\phi_1)$ is used as a detection quantity. The maximum is not achieved in the expression given for ΔT_2 in the Appendix. Therefore, it does not directly quantify the maximum leak rate to be undetected, however, it should serve as a good approximation.

In Fig. 6, the adaptive thresholds are shown for the two detection quantities. As can be seen in both cases, the leaks are detected even though measurements of relative humidity are not used for the detection quantities.

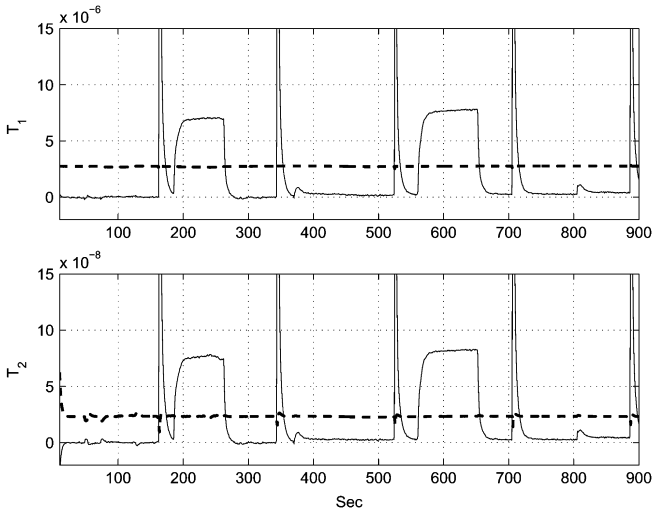

Fig. 6. Simplified detection quantities (solid line) with adaptive alarm thresholds (dashed line). The detection quantities were calculated in both cases with $\phi_1 = 1$.

A number of comments are necessary here. The adaptive thresholds depend on three things principally, the natural leak area of the stack, A_{nl}, anode pressure, p_{an}, and anode temperature, θ_{an}. The dependance on A_{nl} means that if the stack is sealed well, humidity sensors are not necessary as the adaptive threshold would be very small. Intuitively, this makes sense because the detection of leaks becomes strictly a matter of balancing the reacted hydrogen with the flow supplied to the anode. Humidity sensors can, therefore, be omitted if the stack has a small natural leak. The adaptive threshold also depends on the anode pressure. The data presented here were taken for a stack that operates at relatively low pressure (1.2 bar). Stacks designed for high pressure operation (2 bar), to increase the power density, would contain more hydrogen in the stack, in turn requiring a lower threshold. This, on the other hand, could be compensated for by the fact that the operating temperature is often as high as 80 °C. Higher temperature increases the saturation pressure, which in turn increases the adaptive threshold.

The presented analysis shows that when relative humidity sensors are not available for leak detection, the natural leak introduces uncertainty in the hydrogen mass balance equation as the mass fraction of hydrogen in the natural leak is unknown. If relative humidity varies inside the anode, then even when relative humidity measurements are available, as the natural leak location is unknown, uncertainty in the mass balance can be considerable. On the other hand, it has been shown that this uncertainty can be bounded and the bounds used for alarm limits.

If other gases are known to be present in the anode and the upper limits of their partial pressure is known, adaptive alarm limits taking their presence into account can be calculated following the steps presented in this section.

VI. Configurations of Fuel Supply Systems

In Fig. 7, common configurations of hydrogen supply systems for PEM fuel cell stacks are shown, see [6]. The main difference between these configurations and the one presented in Fig. 1 is

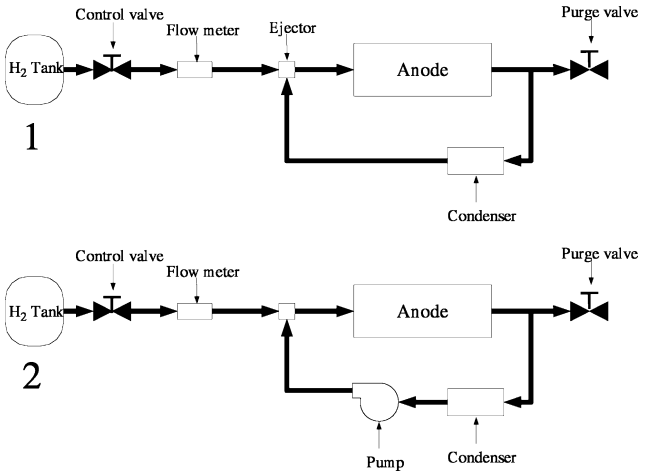

Fig. 7. Common configurations of hydrogen supply systems.

the recirculation system used to increase the mass flow rate of hydrogen through the anode.

The applicability of the presented detection quantities and alarm limits for these configurations would primarily depend on whether the recirculation system could accumulate hydrogen (more hydrogen could enter the system than recirculate back to the anode). If the system could accumulate hydrogen, a false alarm could be sounded as the detection quantities are based on mass balances of hydrogen. Commonly the recirculation systems do not have a large volume, nor are they operated at high pressures, both of which would be necessary for the system to accumulate hydrogen. Therefore, in most cases, the detection quantities could be used for hydrogen leak detection even when recirculation systems are present in the hydrogen supply system.

In fuel cell stacks fed with reformed hydrocarbon fuel (reformate, such as natural gas), there is a high concentration of carbon dioxide and nitrogen in the anode that requires continuous flow through the anode. In this case, a model of the hydrogen mass flow leaving the anode is necessary. Moreover, there is a need for a good adaptive threshold to account for uncertainty in the anode inlet hydrogen composition. Future work will address these issues.

VII. Conclusion

In this brief, model-based hydrogen leak detection for PEM fuel cell systems has been considered. A model for the anode based on mass balances has been presented. The model was used to create two detection quantities which were validated and compared using experimental data where leaks in the anode could be introduced in a controlled manner.

It has been shown how the uncertainty, resulting from the hydrogen mass fraction in the natural leak being unknown, can be bounded and the bound used as an adaptive alarm limit, eliminating false alarms and quantifying missed detections due to the uncertainty. The adaptive alarm limit also serves to eliminate the dependence on relative humidity sensors for hydrogen leak detection. The dependence of this adaptive threshold on natural leak area, pressure and stack temperature was discussed. Finally, the validity of the presented method, when applied to common configurations of hydrogen supply systems, was discussed and motivated.

Appendix

A. Expression for ΔT_1

The analytical expression for ΔT_1, obtained by evaluating (15) with $\phi_1 = 1$ and $\phi_2 = 0$, is

$$\Delta T_1 = A_{\rm nl}\left(\sqrt{\frac{M_{H_2}}{R}} - \frac{M_{H_2}(p_{\rm an} - p_{\rm sat}(\theta_{\rm an}))}{\sqrt{Rp_{\rm an}(M_{H_2}(p_{\rm an} - p_{\rm sat}(\theta_{\rm an})) + M_w p_{\rm sat}(\theta_{\rm an}))}}\right)\lambda.$$

B. Expression for ΔT_2

To obtain an expression for ΔT_2, the following variable is defined:

$$\bar{T} = \frac{dm_{\rm an}}{dt} - \frac{V_{\rm an}}{\theta_{\rm an} R_{\rm an}}\frac{dp_{\rm an}}{dt}. \tag{16}$$

T_2 is then written as $T_2 = \bar{T}/\psi$. The following difference is then evaluated:

$$\begin{aligned} &T_2(\cdot,\phi_1) - T_2(\cdot,\phi_2) \\ &\quad = \frac{\bar{T}(\phi_1)}{\psi(\phi_1)} - \frac{\bar{T}(\phi_2)}{\psi(\phi_2)} \\ &\quad = \frac{\bar{T}(\phi_1)}{\psi(\phi_1)} - \frac{\bar{T}(\phi_2)}{\psi(\phi_2)} - \frac{\bar{T}(\phi_2)}{\psi(\phi_1)} + \frac{\bar{T}(\phi_2)}{\psi(\phi_1)} \\ &\quad = \frac{\bar{T}(\phi_1) - \bar{T}(\phi_2)}{\psi(\phi_1)} + \frac{\bar{T}(\phi_2)}{\psi(\phi_2)}\left(\frac{\psi(\phi_2)}{\psi(\phi_1)} - 1\right) \\ &\quad = \underbrace{\frac{\bar{T}(\phi_1) - \bar{T}(\phi_2)}{\psi(\phi_1)}}_{t_1} + \underbrace{T_2(\phi_2)\left(\frac{\psi(\phi_2)}{\psi(\phi_1)} - 1\right)}_{t_2}. \end{aligned}$$

Notice ΔT_2 is calculated assuming there is no leak in the anode. This in turn should imply that $\Delta A_l = T_2 = \bar{T}/\psi = 0$, meaning $t_2 = 0$ in the equation above. On the other hand, as was explained in Section IV, there is always a small error, so $T_2(\phi_2)$ is assumed to have an upper bound of $\epsilon = A_{\rm nl}/2$ which corresponds to the numerical values given in Section IV. Simplifying the equations for t_1 and t_2 above gives

$$\begin{aligned} t_1 &= A_{\rm nl}\left(\sqrt{\frac{R_{\rm an}(\phi_1)}{R_{\rm an}(\phi_2)}} - 1\right) + \frac{V_{\rm an}}{\lambda\theta_{\rm an}}\frac{dp_{\rm an}}{dt} \\ &\quad \times \left(\frac{\sqrt{R_{\rm an}(\phi_1)}}{R_{\rm an}(\phi_2)} - \frac{\sqrt{R_{\rm an}(\phi_1)}}{R_{\rm an}(\phi_1)}\right) \\ t_2 &\le \frac{1}{2}A_{\rm nl}\left(\sqrt{\frac{R_{\rm an}(\phi_1)}{R_{\rm an}(\phi_2)}} - 1\right) \end{aligned}$$

which, in turn, gives the following expression for ΔT_2, where it has been used that $T_2(\cdot,\phi)$ is monotonic in ϕ:

$$\Delta T_2 = \max_{\phi_1,\phi_2\in[0,1]} T_2(\cdot,\phi_1) - T_2(\cdot,\phi_2)$$
$$\Downarrow$$
$$\Delta T_2 \leq \left[\frac{3}{2}A_{\rm nl}\left(\sqrt{\frac{R_{\rm an}(\phi_1)}{R_{\rm an}(\phi_2)}}-1\right) + \frac{V_{\rm an}}{\lambda\theta_{\rm an}}\frac{dp_{\rm an}}{dt}\left(\frac{\sqrt{R_{\rm an}(\phi_1)}}{R_{\rm an}(\phi_2)} - \frac{\sqrt{R_{\rm an}(\phi_1)}}{R_{\rm an}(\phi_1)}\right)\right]\Bigg|_{\phi_1=0,\phi_2=1}.$$

REFERENCES

[1] L. C. Cadwallader and J. S. Herring, "Safety issues with hydrogen as a vehicle fuel," Idaho Nat. Eng. Environ. Lab., INEEL/EXT-99-00522, Sep. 1999.

[2] J. Alcock, L. Shirvill, and R. Cracknell, "Compilation of existing safety data on hydrogen and comparative fuels," Tech. Rep., Shell Global Solutions, May 2001.

[3] J. Larminie and A. Dicks, *Fuel Cell Systems Explained*. New York: Wiley, 2003.

[4] X. Lu, S. Wu, L. Wang, and Z. Su, "Solid-state amperometric hydrogen sensor based on polymer electrolyte membrane fuel cell," *Sens. Actuators B*, vol. 107, pp. 812–817, 2005.

[5] M. T. S. Nyberg, "Model based diagnosis of the air path of an automotive diesel engine," *Control Eng. Practice*, vol. 12, pp. 513–525, 2004.

[6] P. Rodatz, A. Tsukada, M. Mladek, and L. Guzzella, "Efficiency improvements by pulsed hydrogen supply in pem fuel cell systems," presented at the IFAC World Congr., Barcelona, Spain, 2002.

[7] M. Arcak, H. Görgün, L. M. Pedersen, and S. Varigonda, "A nonlinear observer design for fuel cell hydrogen estimation," *IEEE Trans. Contr. Syst. Technol.*, vol. 12, no. 1, pp. 101–110, Jan. 2004.

[8] J. Pukrushpan, A. Stefanopoulou, and H. Peng, "Control of natural gas catalytic partial oxidation for hydrogen generation in fuel cell aplications," *IEEE Trans. Contr. Syst. Technol.*, vol. 13, no. 1, pp. 3–14, Jan. 2005.

[9] M. Nyberg, "Model based fault diagnosis: Methods, theory, and automotive engine applications," Ph.D. dissertation, Linköping Univ., Linköping, Sweden, Jun. 1999.

[10] J. Pukrushpan, H. Peng, and A. Stefanopoulou, "Control-oriented modeling and analysis for automotive fuel cell system," *J. Dyn., Syst., Meas., Control*, vol. 126, pp. 14–25, 2004.

[11] J. Sun and I. V. Kolmanovsky, "Load governor for fuel cell oxygen starvation protection: A robust nonlinear reference governor approach," *IEEE Trans. Contr. Syst. Technol.*, vol. 13, no. 6, pp. 911–920, Nov. 2005.

[12] W. He, G. Lin, and T. Van Nguyen, "Diagnostic tool to detect electrode flooding in proton-exchange membrane fuel cells," *AIChE J.*, vol. 49, no. 12, pp. 3221–3228, Dec. 2003.

[13] F. Barbir, X. Wang, and H. Gorgun, "Pressure drop on the cathode side of a PEM fuel cell as a diagnostic tool for detection of flooding and drying conditions," in *Proc 3rd Int. Conf. Fuel Cell Science, Engineering, and Technology*, 2005, pp. 25–29.

[14] S. S. Kocha, J. Deliang Yang, and J. S. Yi, "Characterization of gas crossover and its implications in PEM fuel cells," *AIChE J.*, vol. 52, no. 5, pp. 1916–1925, May 2006.

[15] M. Kinnaert, "Fault diagnosis based on analytical models for linear and nonlinear systems—A tutorial," in *Proc. IFAC Safeprocess*, 2003, pp. 37–50.

[16] R. Isermann, "Process fault detection based on modeling and estimation methods—{A} survey," *Automatica*, vol. 20, pp. 387–404, 1984.

[17] T. Höfling and R. Isermann, "Fault detection based on adaptive parity equations and single-parameter tracking," *Control Eng. Practice*, vol. 4, pp. 1361–1369, 1996.

[18] M. Nyberg and M. Krysander, "Combining AI, FDI and statistical hypothesis-testing in a framework for diagnosis," in *Proc. IFAC Safeprocess*, 2003, pp. 891–896.

[19] D. A. McKay, W. T. Ott, and A. G. Stefanopoulou, "Modeling, parameter identification, and validation of water dynamics for a fuel cell stack," presented at the ASME Int. Mechanical Engineering Congr. Expos., 2005.

[20] D. A. McKay and A. G. Stefanopoulou, "Parameterization and validation of a lumped parameter diffusion model for fuel cell stack membrane humidity estimation," in *Proc. IEEE Amer. Control Conf.*, Jun. 2004, vol. 1, pp. 816–821.

[21] P.-Y. A. Chuang, A. Turhan, A. K. Heller, J. S. Brenizer, T. A. Trabold, and M. Mench, "The nature of flooding and drying in polymer electrolyte fuel cells," presented at the ASME Conf. Fuel Cell Science, Engineering and Technology, 2005.